Article
Vol. 25, No. 1, p. 59–70, February 2021
https://doi.org/10.1007/s12303-020-0049-0
pISSN 1226-4806 eISSN 1598-7477
Geosciences Journal GJ

The relationships among faults, geology and geophysical data in the southwestern Korean Peninsula, including the Haenam area, and their application for the interpretation of earthquakes

Yong-seok Jang[1] and Chang-whan Oh[2]*

[1]The Earth and Environmental Science System Research Center, Jeonbuk National University, Jeonju 54896, Republic of Korea
[2]Department of Earth and Environmental Sciences, Jeonbuk National University, Jeonju 54896, Republic of Korea

ABSTRACT: The southwestern Gyeonggi Massif features many faults. The main faults are NE-striking faults, including the Jeonju and Kwangju faults, and they are cut by N-S- and NNE-striking faults. Additionally, E-W-, WNW-, and NW-striking faults occur as minor faults. Historical earthquakes with magnitudes greater than 5.0 have occurred on or near these faults. Earthquakes with focal depths shallower than 12 km have generally occurred on the NE-, NNE-, and N-S-striking faults, while those with hypocenters deeper than 12 km have occurred on the NW-, WNW-, and NE-striking faults or do not show a relationship with any faults. The instrumental earthquakes with magnitudes greater than 5.0 in the Korean Peninsula mainly have hypocenters deeper than 12 km, and their epicenters form a NW-oriented trend. These data effectively reflect two seismogenic layers with a boundary at ca. 12 km, as suggested in a previous study. The recent earthquake in the Haenam area occurred in the lower seismogenic layer. The shallower earthquakes seem to be the result of the reactivation of pre-existing faults. In comparison, the deeper earthquakes tend to occur on recently formed or newly formed faults related to the present regional stress of the Korean Peninsula. The shear-wave velocity tomography of the southwestern Gyeonggi Massif at 1 km corresponds well to the geology. In contrast, the shear-wave velocity variations at 5–9 km generally correspond to the locations of brittle faults. The depth of the ~3.5 km/s isovelocity line is quite irregular and is deeper in areas with active fault movement. In the Gyeongsang basin, the relationship between the shear-wave velocity and faults is somewhat unclear because the thickness of low-density sedimentary rocks is up to 8 km. Shear-wave velocity tomography at 13 km can be used to identify areas with high shear stress. These data indicate that shear-wave velocity tomography may provide different information depending on the depth and that the brittle faults in this region may not extend to a depth of 13 km.

Key words: earthquake, fault, shear-wave velocity, tomography, southwestern Korean Peninsula

Manuscript received August 28, 2020; Manuscript accepted November 15, 2020

1. INTRODUCTION

The Korean Peninsula, unlike regions located at plate boundaries such as Japan, has been considered a seismically stable area because it is located inland far from plate boundaries, such as subduction zones (Lee and Yang, 2006). However, in the Gyeongju and Pohang areas, earthquakes with magnitudes equivalent to 5.8 and 5.4 have occurred recently (Woo et al., 2019; Kim et al., 2020; Jin et al., 2020). In addition, the Pohang earthquake confirmed that an earthquake with a magnitude of 5.4 could cause severe damage in areas where the ground is weak (Kim et al., 2020). This event reminds us that the Korean Peninsula is not immune to the impacts of earthquakes. In addition, the magnitude and frequency of earthquakes are increasing worldwide (Choi and Kim, 2018), which also increases the risk of earthquakes on the Korean Peninsula. The increased risk of earthquakes caused by these natural factors is amplified by the construction of many hazardous large-scale facilities, such as nuclear power plants and hazardous materials and gas storage sites, in the Korean Peninsula.

Many historical earthquakes have been recorded on the Korean Peninsula, and in some cases, the magnitude of the

*Corresponding author:
Chang-whan Oh
Department of Earth and Environmental Sciences, Jeonbuk National University, 567 Baekje-daero, Deokjin-gu, Jeonju 54896, Republic of Korea
Tel: +82-63-270-3395, E-mail: ocwhan@jbnu.ac.kr

historical earthquake exceeded 7.0 (Houng and Hong, 2013). Although researchers have different opinions about the maximum magnitude of earthquakes that can occur on the Korean Peninsula, some researchers have suggested that earthquakes can reach magnitudes of 7.2–7.4 (Lee and Na, 1983; Lee and Jin, 1991; Lee, 1998; Hong et al., 2018). Existing domestic nuclear power plants are designed to tolerate earthquakes of up to 6.5 magnitude, and new nuclear power plants that are being built are designed to tolerate earthquakes of up to 6.9–7.0 magnitude (Choi and Kim, 2018). Therefore, it is impossible to rule out the potential for a nuclear disaster caused by an earthquake on the Korean Peninsula. Such a disaster could create a severe crisis in large cities such as Busan and Ulsan and could cause issues that could sink the Korean economy.

In the long term, it is necessary to train many experts and invest considerable research funds to improve the research on earthquakes on the Korean Peninsula. It is also essential to determine the best way to enhance the research capacity of the Korean geological community in the near future. Domestic research on earthquakes has focused mainly on geophysics, and joint research between geophysics and other geological fields has been very limited. Since research on earthquakes is a comprehensive geological study, joint research among various geological fields centered on geophysics can increase the ability of earthquake interpretation quickly and solve the problem of a shortage of experts in the near future.

In this study, a shear-wave velocity model and instrumental and historical earthquake information from the southwestern part of the Korean Peninsula, including the Haenam area, are interpreted by linking them with structural, tectonic, and petrologic information. The relationship between earthquakes and faults was investigated by comparing the instrumental and historical earthquake information with information on faults in the study area. The shear-wave velocities at different depths were interpreted by comparing the shear-wave velocity data with geologic, fault distribution, and tectonic data. We also try to understand the implications of the recent Haenam earthquakes.

2. GENERAL GEOLOGY

The Korean Peninsula consists of three main massifs, the Nangrim Massif, Gyeonggi Massif (GM), and Yeongnam Massif (YM), from north to south (Chough et al., 2000; Lee et al., 2001; Oh et al., 2018). The GM and YM are separated by the Okcheon Fold Belt (OFB), which extends northeastwards from the Mokpo–Haenam area to the Taebaeksan area. The OFB is divided into the Okcheon Metamorphic Belt (OMB) and Taebaeksan Basin (TB). Due to the regional intrusion of Jurassic granitoids, the

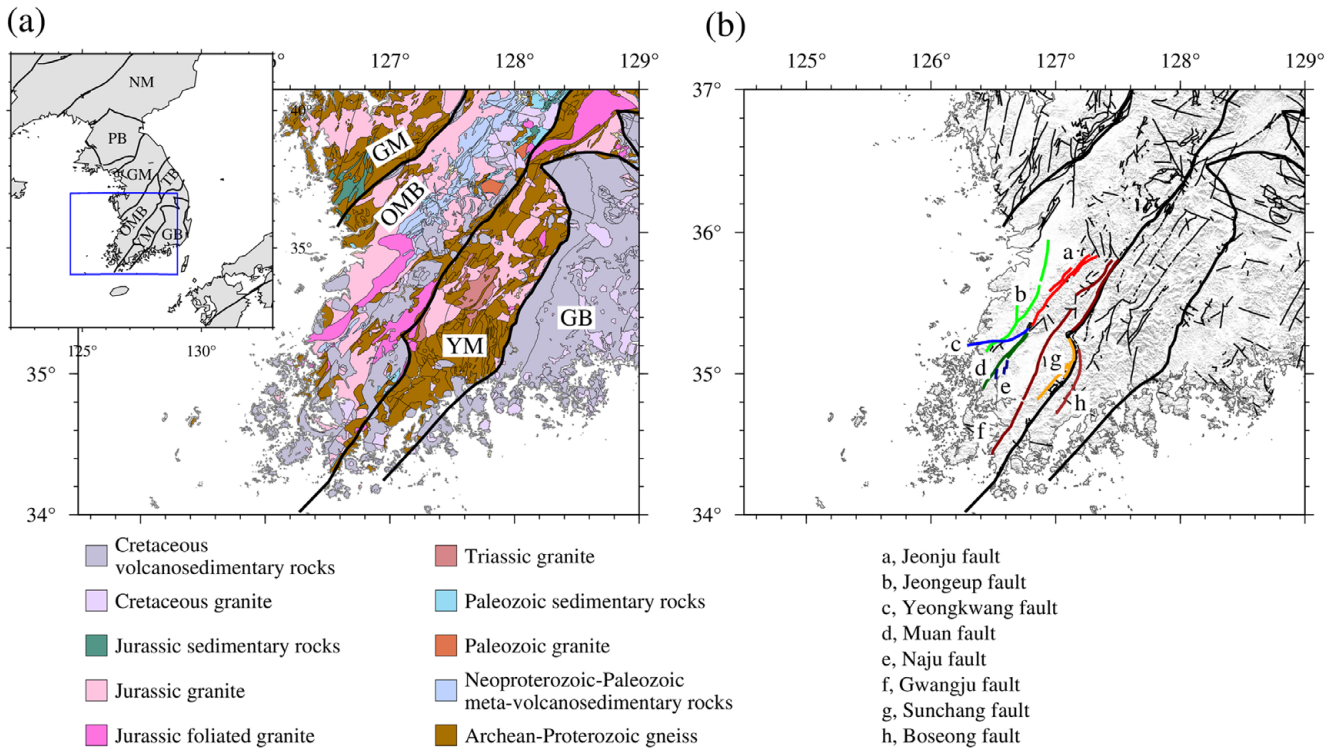

Fig. 1. Maps of the simplified geology and faults in the southwestern Korea Peninsula. (a) Simplified tectonic maps of the Korean Peninsula and the southwestern Korean Peninsula with tectonic boundaries denoted by solid black lines. (b) Simplified fault map of the southwestern Korean Peninsula. The Okcheon Fold Belt (OFB) consists of the OMB to the southwest and TB to the northeast. NM, Nangrim Massif; PB, Pyeongnam Basin; GM, Gyeonggi Massif; OMB, Okcheon Metamorphic Belt; TB, Taebaeksan Basin; YM, Yeongnam Massif; GB, Gyeongsang Basin.

OMB mainly consists of Jurassic granites with remnants of the original Neoproterozoic–Paleozoic metavolcano-sedimentary rocks in the central part of the OMB (Fig. 1). The southwestern Korean Peninsula consists of the GM, YM, and OMB.

The GM and YM consist of Paleoproterozoic metagranitoids and paragneisses (Lee et al., 2014, 2019; Yengkhom et al., 2014). The OMB mainly consists of Paleozoic metasedimentary rocks with minor Neoproterozoic metavolcano-sedimentary rocks (Oh et al., 2004). During the Permo-Triassic continental collision between the northern and southern portions of the GM, which can be correlated to the North China Craton (NCC) and South China Craton (SCC), respectively, subduction started along the southern margin of the Korean Peninsula and the SCC for the following reasons (Oh, 2006; Oh and Kusky, 2007; Oh, 2012). During Permo-Triassic time, the southern Korean Peninsula and the SCC could no longer move northwards due to the collision with the NCC; consequently, the oceanic crust, which was also moving northwards, began to subduct beneath the Korean Peninsula and the SCC. This subduction continued until the Jurassic, forming an arc along the southern margin of the Korean Peninsula and the SCC with the intrusion of subduction-related igneous rocks from Permian to Jurassic time (Hu et al., 2015). The subduction-related igneous activity was not strong during the Permian but became pervasive starting in the Triassic (Yi et al., 2012). As a result, Triassic igneous rocks are abundant in the YM (Kim et al., 2011; Zhai et al., 2016). Starting in the Jurassic, the position of the arc moved northwards in response to a decrease in the subduction angle, resulting in abundant Jurassic granites in the OMB and the GM (Kee et al., 2010; Kim et al., 2011). During the early to middle Jurassic, a northeast-trending strike-slip fault with ductile dextral movement developed, resulting in the Honam shear zone and mylonitizing the surrounding Jurassic granites (Kim et al., 2006). At approximately 160 Ma, the arc-related igneous activity stopped due to flat subduction of the Paleo-Pacific plate under the eastern Asian continent (Kim et al., 2016).

In the early Cretaceous, regional extension occurred in eastern Asia, forming Cretaceous basins in many localities in eastern Asia (Zhou and Li, 2000; Li et al., 2019; Wu et al., 2019; Lee et al., 2020). The extension was caused by the rollback of the subducted oceanic slab towards the Pacific Ocean side and resulted in upwelling of the asthenospheric mantle. This upwelling caused extensive igneous activity due to the melting of the lithosphere by the heat supplied by the upwelling asthenospheric mantle and partial decompression melting of the asthenospheric mantle. In the mid-Cretaceous, the deep Honam shear zone that formed during the Jurassic was uplifted to the surface or near-surface along with large Jurassic batholiths. The extension continued into the middle Cretaceous, and brittle sinistral strike-slip movement occurred roughly along the Honam shear zone. This sinistral strike-slip movement resulted in many pull-apart Cretaceous basins, such as the Jinan, Muju, and Yeongdong basins along the Jeonju-Kwangju fault system and the Iksan-Gongju fault system in the southern Korean Peninsula. Additionally, the Gyeongsang basin (GB) also formed at this time due to extension or oblique subduction (Lee, 1999; Lee et al., 2020). As a result, Cretaceous volcano-sedimentary sequences were deposited in these basins, and Cretaceous volcanic activity occurred along the faults and boundaries of these basins.

3. THE EVOLUTION OF FAULTS AND ACTIVE FAULTS IN THE STUDY AREA

The main faults in the study area located in the southwestern Korean Peninsula are as follows. The Jeonju and Gwangju faults are the main faults with NE strikes (Fig. 1b; Choi et al., 2011). The Jeonju fault extends from the Mokpo area to the Yongdam area, and its southwestern segment is called the Muan fault. The Jeongeup fault is almost parallel to the Jeonju Fault, and the E-W-striking Yeongkwang fault appears to be a branch of the Jeonju fault. The Gwangju fault extends from the Haenam area to the Jinan area. The Naju fault has a N-S strike and may cut the southwestern part of the Jeonju fault. The Jeonju and Kwangju faults are cut and segmented by N-S-striking faults. In the eastern part of the study area, several faults with NE strikes, including the Boseong fault, are cut by faults with N-S or NNE strikes. The Sunchang fault is one of the faults with a NNE strike and connects to the Gwangju fault via a curved fault. The faults with NE strikes are also cut by faults with NW strikes, which are abundant in the northeastern part of the study area and occur along with WNW- or E-W-striking faults in the southwestern margin of the study area, including the Haenam area. These distribution patterns of faults suggest that the NE-striking fault formed earlier than the N-S- and NNE-striking faults. Although further study is needed, the NW-, WNW-, and E-W-striking faults appear to be the youngest faults.

The strike-slip faults with NE strikes show dextral movement and deformed Jurassic igneous rocks with ages older than 180–160 Ma, suggesting that they formed at approximately 180–160 Ma (Cho et al., 1999; Kim et al., 2011). Some of the deformed rocks are mylonites that reflect ductile fault movement at great depth. The Honam shear zone was formed by ductile dextral faulting along NE strike-slip faults (Cho et al., 1999). During 180–160 Ma, the study area may be an arc front, and the ductile dextral fault may have been caused by the compression resulting from oblique subduction of the Paleo-Pacific plate or by ridge subduction, similar to the process forming the San Andreas fault in California (Sagong et al., 2005). The Honam shear zone and

https://doi.org/10.1007/s12303-020-0049-0

Jurassic batholiths that formed in the deep part of the arc may have been uplifted to the surface or near-surface in the early or middle Cretaceous. This inference is supported by the presence of Jurassic granitoid fragments in middle Cretaceous sediments. The NE-directed faults near the surface were reactivated during the middle Cretaceous, resulting in brittle faults with a sinistral sense of movement (Lee, 1990). Many pull-apart basins, including the Jinan and Yeongdong basins, formed between these sinistral NE-striking faults (Lee, 1990; Ryang, 2013). These sinistral faults were caused by the oblique subduction of the Paleo-Pacific oceanic plate. The movement direction along the NE-striking faults changed to dextral again in the Cenozoic, but it is not clear when and why the dextral slip occurred. Possible reasons for the dextral movement include the eastward compression caused by the collision along the Himalayan collisional belt and the compression induced by the oblique subduction of the Paleo-Pacific oceanic plate.

The active faults in the study area were investigated by Choi et al. (2011). That study identified three active faults. One is the Bibong fault with a NE strike (N50°E/85°SE), which developed at 270 ± 15 ka at N36°01′70″ and E127°07′025″. The others are the Gui fault and the Yongdam fault. The N-S-striking Gui fault (N-S/60°W) cuts the Jeonju fault and formed at 130 ± 5 kb at N35°47′13″ and E127°23′02″. The Yongdam fault (N20°E/65°SE) formed near the northeastern part of the Gwangju fault (N35°55′49″ and E127°27′43″) at 420 ± 45 ka. Recently, in the Haenam area, WNW-striking faults (N9°E/65°SE) were found to have strikes and trends similar to those of fault planes acquired from seismic records (Kee, 2020).

These data indicate that the NE-striking strike-slip faults formed with a ductile dextral sense in the early Jurassic at great depth and then underwent brittle sinistral strike-slip movement at a shallow depth during the Cretaceous. Finally, the NE-striking faults were reactivated with brittle dextral movement during the Cenozoic. The NE-striking strike-slip faults were then cut by the N-S-, NNE-, and NW-striking faults. The previous study shows that in the southwestern part of the Korean Peninsula, active faults developed through reactivation of the pre-existing NE-, N-S-, and NNE-trending faults within the last 500 ka due to the present tectonic stress on the Korean Peninsula. Research by KIGAM on the Haenam area found that the WNW faults caused earthquake (Kee, 2020).

4. THE RELATIONSHIP BETWEEN EARTHQUAKES AND FAULTS

The distributions and magnitudes of earthquakes were carefully examined by plotting them on the fault map to investigate the relationship between earthquakes and faults (Fig. 2). Information on instrumental and historical earthquakes is provided by the National Earthquake Center (NECIS, National Earthquake Comprehensive System), and we used the origin time (UTC), location, magnitude, intensity, and focal depth data. In total, this study uses ~10,000 instrumental earthquakes, ranging from August 1978 to July 2020, and ~2,100 historical earthquakes. The focal depth data for the instrumental earthquakes can be acquired from 2016 to 2020, and the number of data points is ~7,000. Figure 2a shows the epicenters of the instrumental earthquakes. Earthquakes larger than magnitude 3.0 were the focus of this study since those below magnitude 3.0 are so scattered that it is not easy to determine any trend in the spatial distribution. The historical earthquakes are also plotted to obtain a more reliable interpretation of the seismicity in the region (Fig. 2b). The precision of locations and magnitudes (intensity) of the historical earthquakes are uncertain because they were reconstructed later based on historical records. However, historical earthquakes are essential for research on the seismicity in the study area because they span a much longer period (~1,500 years) than the ~40 years of instrumental earthquakes. The intensity of the historical earthquakes is converted to magnitude using an empirical equation suggested by Kim and Kyung (2015) for a reliable comparison with instrumental earthquakes. The applied equation is $M_L = 1.7 + 0.571I_0$, where M_L is the magnitude of a local earthquake and I_0 is the epicentral intensity.

Although the relation between epicenters and faults is not easy to deduce for either instrumental or historical earthquakes, most instrumental earthquakes larger than magnitude 3.0 and historical earthquakes with magnitudes larger than 4.0 are observed on or near faults (Figs. 2a and b). In particular, the relationship between earthquakes and faults is clearer for historical earthquakes with magnitudes larger than 5.0, and locations with multiple historical earthquakes are located on faults (Fig. 2b). In the Honam area, historical earthquakes with magnitudes larger than 4.0 and instrumental earthquakes with magnitudes larger than 3.0 have occurred on or near the Jeonju and Kwangju faults, and some earthquakes with magnitudes larger than 3.0 have occurred on the Jengeup fault. Historical earthquakes with magnitudes larger than 5.0 in the northern GB and the Songrisan area appear to occur on NW-directed faults. However, some instrumental earthquakes with magnitudes of 3.0 or less show associations with faults, while others do not. This is likely because the associated small faults have not yet been identified.

Earthquake occurrence density maps are shown in Figures 2c and d. The study area was divided into 20 km × 20 km unit areas, and the earthquake occurrence density contours within the study area were drawn using the total number of earthquakes occurring within each unit area. The earthquake occurrence density map for the instrumental earthquakes (Fig. 2c) does not show a clear

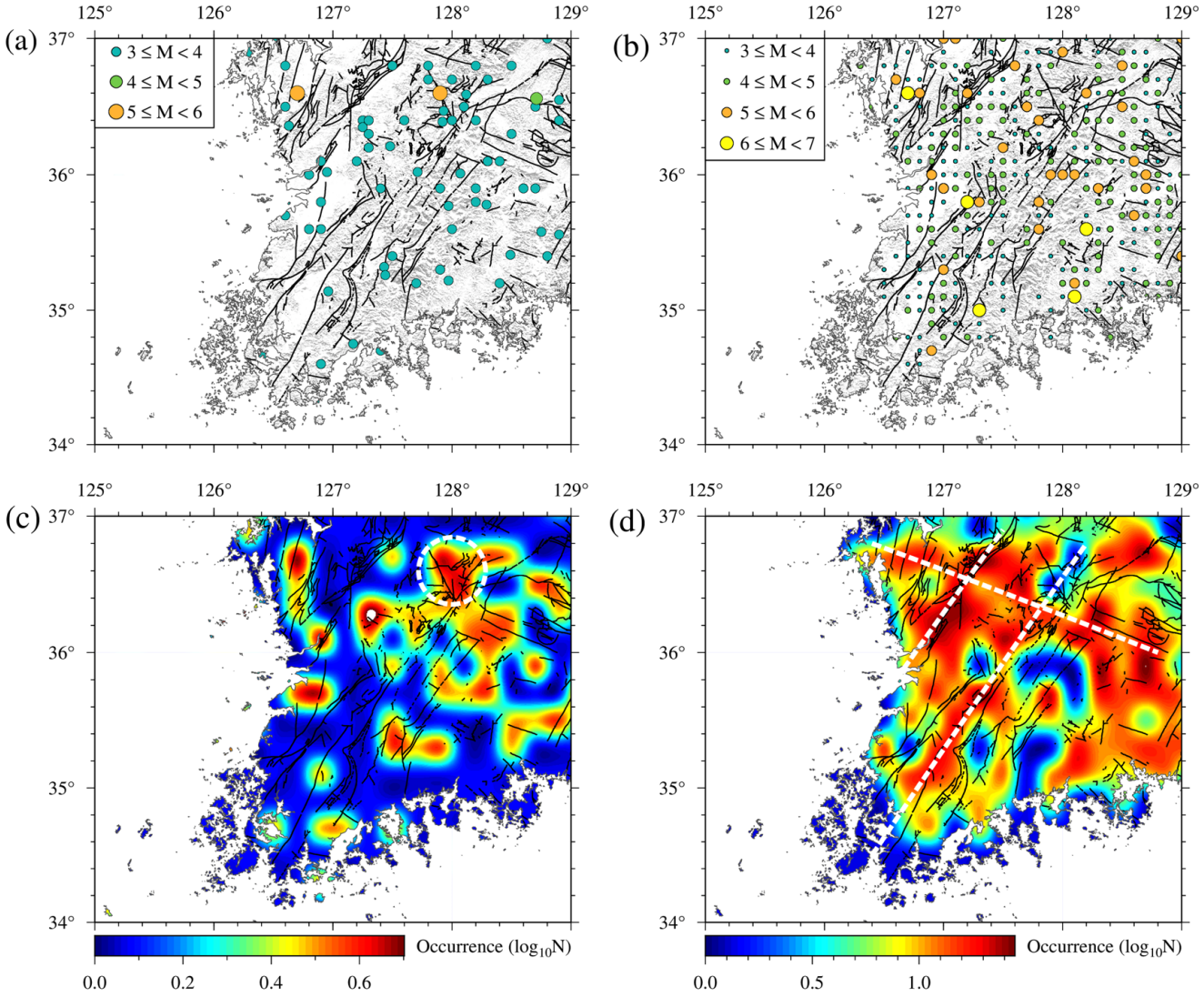

Fig. 2. Earthquake distribution maps. Distribution maps of instrumental and historical earthquakes are shown in (a) and (b), respectively. Earthquake occurrence density maps of the instrumental and historical earthquakes are shown in (c) and (d). The circle in (c) denotes the location of the maximum occurrence density of instrumental earthquakes, and the white lines in (d) indicate major earthquake occurrence trends recognized from historical earthquakes.

relationship between earthquakes and faults, but regions with high earthquake density are located in regions with many faults, such as the northern part of the OMB, and do not appear well in areas without faults (Figs. 1a and 2c). On the other hand, in the historical earthquake density map, the areas with more than 10 historical earthquakes show some of relationships with faults (Fig. 2d). Although not particularly clear, most areas with high earthquake densities appear in three belts. Two belts are the NE-directed Jeonju-Gwangju fault system, which connects the Mokpo–Haenam and Jinan–Muju areas, and the NE-directed Gongju fault system, which connects the Iksan and Gongju areas. Additionally, the third belt connects Uuiseong and Hongseong and features a NW orientation similar to the NW-striking faults in the Uuiseong area. This earthquake zone with a NW orientation seems to extend into the Gyeongju and Pohang areas to the southeast and into the Baengnyeongdo area to the northwest. Along this zone, instrumental earthquakes with magnitudes greater than 5 have occurred in the Baengnyeongdo, Hongseong, Songrisan, Gyeongju and Pohang areas (Kang and Baag, 2004; Lee, 2010; Kim et al., 2016; Kim et al., 2020).

5. SHEAR-WAVE VELOCITY

The 3D shear-wave velocity model produced by Jung et al. (2011) is adopted for the investigation of the relationship between faults and shear-wave velocity. The 3D shear-wave velocity model was built by combining two data sets: Rayleigh waves between 0.1 s and 1.2 s and Rayleigh waves between 1.0 s and 10 s. The former

https://doi.org/10.1007/s12303-020-0049-0

was provided by crustal-scale refraction experiments, and the latter was estimated using natural earthquakes. By combining the two data sets, Rayleigh wave dispersion data at periods between 0.1 s to 10 s were reconstructed and then inverted into a shear-wave model extending to 12 km depth. The Rayleigh wave dispersion data at every single grid point were inverted into shear-wave velocities by using the surf96 program of Herrmann and Ammon (2002). The 0.1° × 0.1° tomographic cell size was verified with checkerboard tests composed of 0.4° × 0.4° square blocks. On the Korean Peninsula, a limited number of tomographic inversion images were made using surface wave data (e.g., Kang and shin, 2006; Choi et al., 2010). They used cell sizes similar to those in this study and showed results very similar to those of our study. However, the model of Jung et al. (2011) has an advantage over previous studies in the broader-period range, which caused an increase in vertical resolving power.

Figure 3 shows shear-wave velocity models with faults at depths of 1 km, 5 km, 9 km, and 13 km. The shear-wave velocities increase with depth, and the average velocity difference from the surface to 12 km depth is ~0.5 km/s. The velocity perturbation weakens with increasing depth; perturbations of 0.50 km/s, 0.33 km/s, 0.20 km/s, and 0.10 km/s are observed at 1 km, 5 km, 9 km, and 13 km, respectively. Higher shear-wave velocities were observed from 1 to 13 km in the Yeongnam massif, which consists of

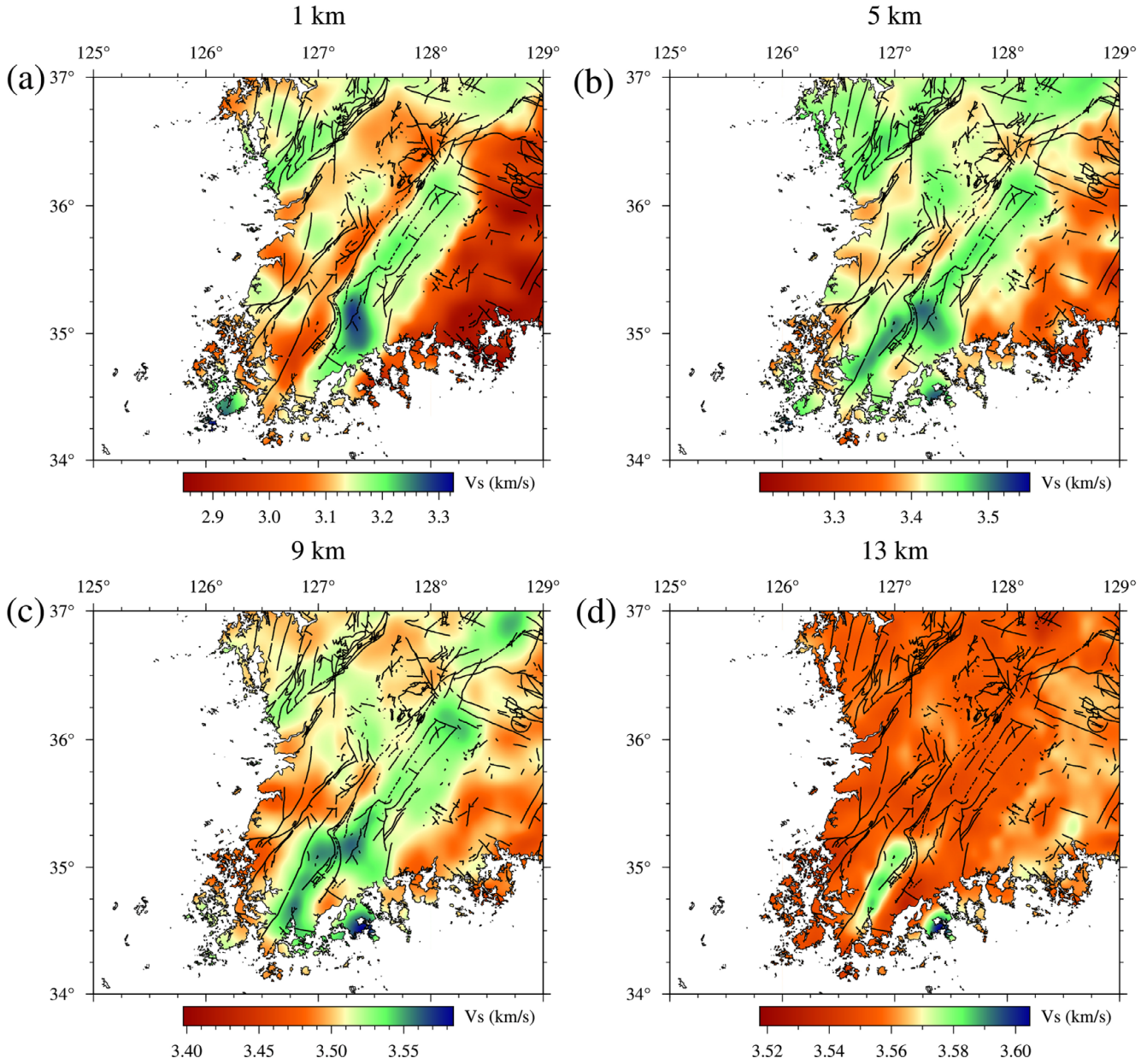

Fig. 3. Horizontal shear-wave velocity maps at depths of 1, 5, 9, and 13 km in the study area.

Paleoproterozoic gneisses and Triassic–Jurassic granites. The shear-wave velocity distribution at 1 km depth shows a close relationship with the surface geology of the study area (Fig. 3a). Low shear-wave velocities are observed in the areas consisting of sedimentary basins, such as the GB and the OMB within the OFB, and the Cretaceous volcano-sedimentary pull-apart basins along the Jeonju-Kwangju fault system. In contrast, high shear-wave velocities are observed in the YM and in the areas consisting of gneiss and granite within the GM and OMB. Therefore, the low velocities at a depth of 1 km represent areas consisting of low-density materials, such as sedimentary rocks, while high velocities represent areas consisting of high-density materials, such as gneiss and granite.

The shear-wave velocity maps at depths of 5 and 9 km show a decrease in the velocity contrasts compared to that at 1 km depth in the southwestern Korean Peninsula. Depths of the volcano-sedimentary pull-apart basins along with the Jeonju-Kwangju fault system and the depth of the metasedimentary basin in the OMB were estimated to be less than ~3.0 km (Lee, 1999; Park and Song, 2011). Therefore, at depths below 5 km, the southwestern Korean Peninsula can be considered to be composed of a basement consisting of gneiss and granite, similar to the YM. As a result, the velocity contrast decreases at depths of 5 and 9 km. The areas showing low shear-wave velocities at depths of 5 and 9 km match the areas with faults rather well. On the other hand, in the GB, the shear-wave velocity contrast at depths of 5 and 9 km does not decrease, and the shear velocities are still low without showing a relationship with faults. The depth of sedimentary rocks in the GB can reach up to ~8 km (Min and Chung, 1985; Kim, 1999; Choi et al., 2009), suggesting that the low and homogenous shear velocities in the GB at depths of 5 and 9 km may be related to the thick sediments in the GB.

The velocities of most areas at 13 km depth are ~3.55 km/s, except the areas around the Sunchang fault, which show a velocity of ~3.58 km/s. The relationship between shear-wave velocities and faults is not observed at this depth, suggesting that the brittle faults do not continue to this depth. The high and relatively homogeneous velocities at 13 km depth represent the basement, which consists mainly of gneiss or granites. Therefore, the high velocity around the Sunchang fault indicates high shear stress. Higher velocities around the Sunchang fault are also observed in the shear-wave velocity maps at depths of 1, 5, and 9 km. The epicenter of a historical earthquake larger than magnitude 6.0 is also located near the Sunchang fault. These data suggest that a more detailed study will be needed to determine whether the southern part of the Sunchang fault has the potential to produce earthquakes

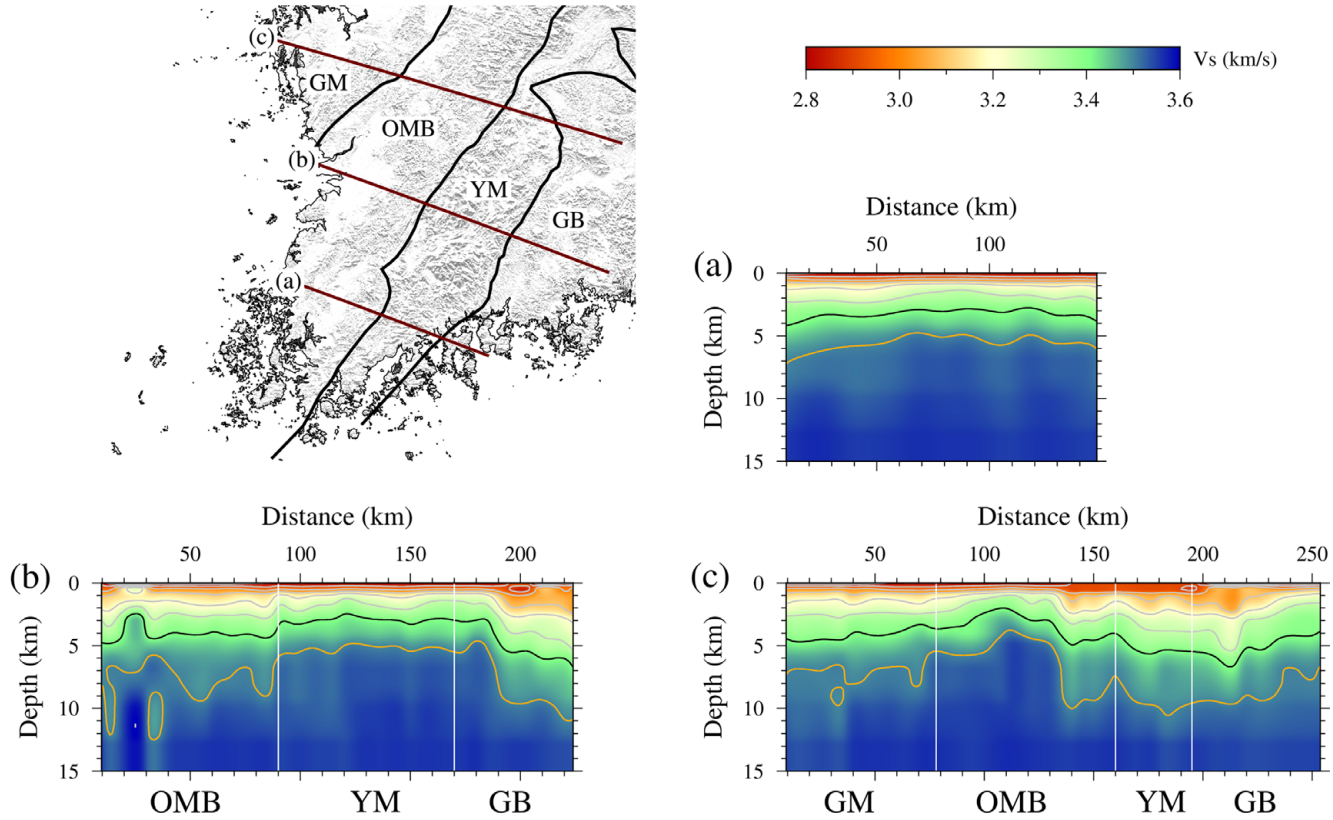

Fig. 4. Vertical shear-wave sections traversing the study area. The brown lines in the map represent the locations of three sections. (a), (b), and (c) represent the vertical sections. The isovelocity lines of 3.4 km/s and 3.5 km/s in the vertical sections are denoted by black and orange lines, respectively. The abbreviations are the same as those in Figure 1.

https://doi.org/10.1007/s12303-020-0049-0

with magnitudes larger than 6.0 in the future.

Vertical shear-wave velocity sections traversing the study area in the NW direction are shown in Figure 4. The vertical sections cross the different tectonic units of the southwestern Korean Peninsula, such as the southwestern GM, OMB, YM, and western GB. The vertical sections are drawn down to 15 km. The isovelocity contours of 3.4 km/s and 3.5 km/s are denoted by black and orange lines, respectively, and gray lines indicate other isovelocities with 0.1 km/s intervals. The shear-wave velocities of the vertical sections clearly show a rapid increase to 3.4 km/s and then a gradual increase to 3.5 km/s. Below the depth with the shear-wave velocity of 3.5 km/s, the velocity change is small, and the velocities do not exceed 3.6 km/s. The average shear-wave velocity of the uppermost crust in the southern Korean Peninsula is < 3.4 km/s (Jung et al., 2007; Cho et al., 2013). The 3.4 km/s isovelocity line in section (a) is distributed between 3 and 4 km, and the depth of the line is slightly deeper in the western margin (Fig. 4a). The ~3.5 km/s isovelocity line is distributed between 5 and 6 km with a slightly deeper depth in the western margin. In section (b), the 3.4 and 3.5 km/s isovelocity lines beneath the YM are located at shallower depths (3 km and 6 km depth, respectively) than those in other tectonic units (Fig. 4b). Under the GB, the 3.4 km/s and 3.5 km/s isovelocity lines are located between depths of 5.5 and 7 km and between depths of 9.5 and 11 km, respectively. Under the OMB, the depth of the 3.4 km/s isovelocity line is rather constant (4.5 km), but the depth is 2.5 km in some narrow areas, whereas the depth of the 3.5 km/s isovelocity line is quite variable from 6–12 km. In Figure 4c, the 3.4 km/s isovelocity line is located at a shallower depth in the western OMB (2.5–3.0 km), at a deeper depth in the eastern OMB, YM, and GB (4–6.5 km), and at a moderate depth in the GM (3.5–4.5 km). The 3.5 km/s isovelocity line also shows a similar pattern in which the line is located at a shallower depth (4–5 km) in the western OMB, at a deeper depth in the eastern OMB, YM, and GB (7–10 km), and at moderate depth in the GM (6–9.5 km).

6. DISCUSSION

6.1. Spatial Distribution of Earthquakes and their Relationship with Faults

Chung et al. (2018) suggested that depth-dependent seismicity exists in the southern Korean Peninsula. They calculated the focal depths of earthquake clusters associated with the Gyeongju and Pohang earthquakes. They found upper and lower seismogenic layers that have different levels of seismicity with a boundary at ca. 12 km. Relatively small earthquakes (M < 3.0) are dominant in the upper seismogenic layer. Moderate to large earthquakes (M > 3.0) are dominant in the lower seismogenic layer. The occurrence of earthquakes is more frequent in the upper layer than in the lower layer.

In this study, we found that the spatial distribution of earthquakes generally shows a correlation with that of faults (Fig. 2). Here, the instrumental earthquakes are divided into two groups based on focal depth according to Chung et al.'s study (2018) and plotted on the fault map (Fig. 5). Many earthquakes with focal depths of less than 12 km (hereafter called shallower earthquakes) are located on or near NE-striking faults. This trend is more evident for earthquakes with focal depths of less than 8 km. The shallower earthquakes have occurred along the northern Jeonju fault, the northern Kwangju fault, and along NE-striking faults in the YM. In addition, shallower earthquakes showing linear NE-oriented patterns are present in the southwestern part of the GB (Fig. 5a). Many earthquakes with focal depths deeper than 12 km (hereafter called deeper earthquakes) do not show a good relationship with fault locations. However, some deeper earthquakes are associated with not only NE-striking faults but also NW-striking faults in the northern GB close to the Gyeongju and Pohang areas (Fig. 5b). The deeper earthquakes seem to be more dominantly associated with NW-striking faults than with NE-striking faults.

Figure 5c shows the relationship among the magnitude, occurrence frequency, and focal depth of the instrumental earthquakes. The following processes were carried out to construct Figure 5c. First, the magnitude vs. occurrence frequency histogram was calculated at 1 km, and then the Gaussian fit of the histogram was estimated. The same procedure was conducted from 2 to 24 km with a 1 km interval. A 3D data set (focal depth-magnitude-earthquake frequency) was built by stacking the resulting data. The 3D data set was expressed in a 2D plane by converting the earthquake frequency into a contour diagram. The average magnitudes of the shallower earthquakes (with focal depths less than 12 km) decrease from 1.6 to 1.1 with increasing depth. In contrast, the average magnitudes of the deeper earthquakes increase from 1.1 to 1.6. The occurrence frequency of shallower earthquakes increases as focal depth increases, and the reverse phenomenon is observed for deeper earthquakes. These results confirm the existence of the two seismogenic layers suggested in this study and the previous study of Chung et al. (2018). These data suggest that shallower earthquakes are more likely to occur along faults with a NE strike and that deeper earthquakes tend to occur along faults with a NW strike. It is, however, difficult to generalize our findings because the NW-striking faults are not well investigated.

The locations of the recent Haenam earthquake cluster are shown in Figure 5d with suggested WNW- and NW-striking faults (Kee, 2020). The maximum local magnitude of the earthquake cluster is 3.2, and the focal depths are between 20 and 23 km.

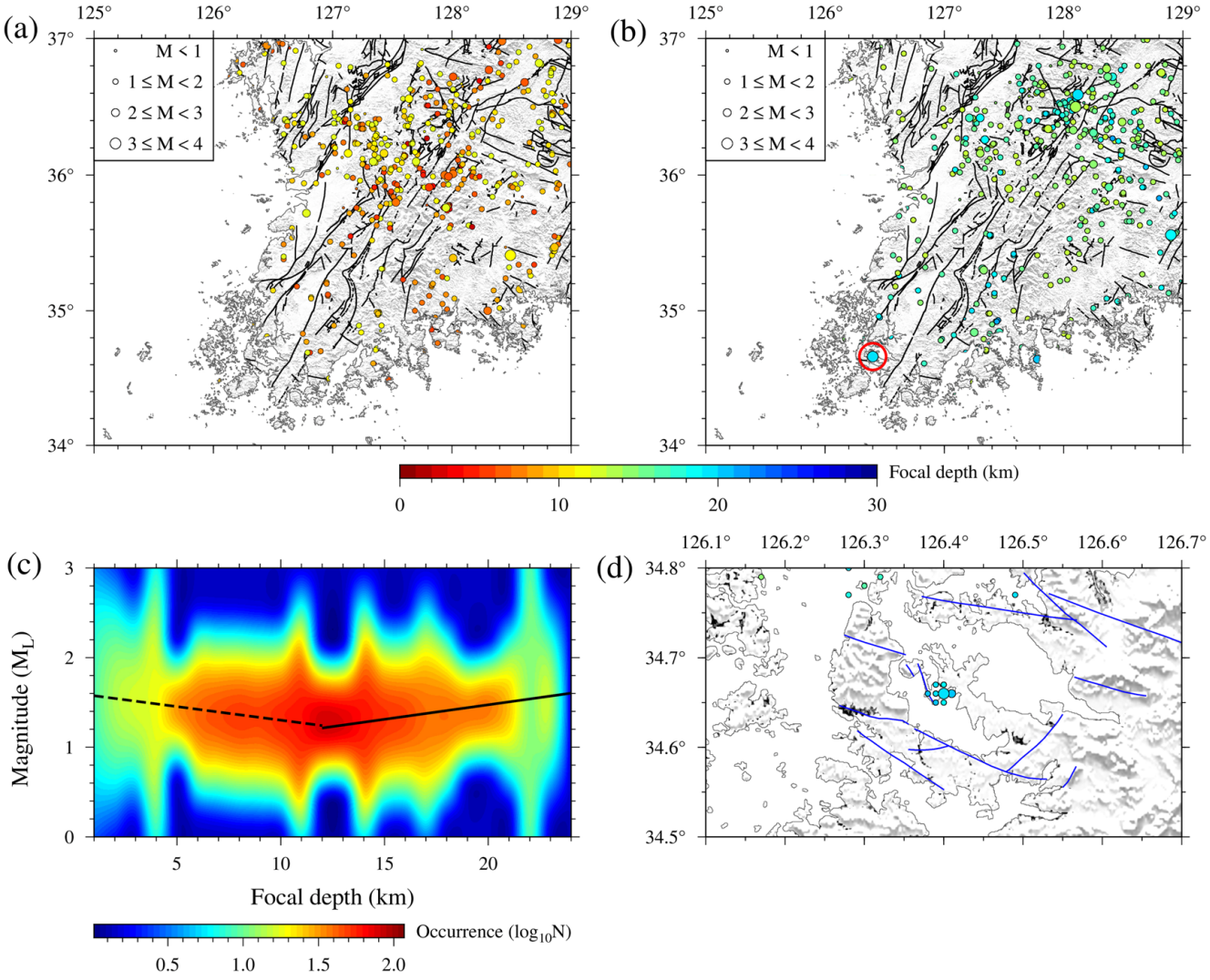

Fig. 5. Distribution maps of the focal depths of instrumental earthquakes (after 2016). The distribution of earthquakes with focal depths shallower than 12 km (a) and the distribution of earthquakes with focal depths deeper than 12 km (b). A contour map of the earthquake occurrence frequency on a focal depth vs. the magnitude diagram (c). The trends of changing magnitude with depth for earthquakes with focal depths shallower and deeper than 12 km are shown by dashed black and black lines, respectively. The Haenam area is denoted by a red circle in (b), and the locations of the WNW- and NW-striking faults (blue lines) surveyed by Kee (2020) and recent instrumental earthquakes in the Haenam area are shown in (d).

The earthquakes in the Haenam area remain a hot topic since there was no pre-existing earthquake record. The geological survey performed after the earthquakes suggested that the earthquake cluster in the Haenam area was associated with strike-slip fault movement along WNW-trending faults. When considering the results in this study, the Haenam earthquakes were caused by fault activity in the lower seismogenic layer at depths greater than 12 km.

6.2. The Different Implications of Shear-wave Velocity with Depth

Various velocity models of the southern Korean Peninsula have been proposed in recent decades, and they show good agreement with each other in terms of the depth of the Moho and the average velocities of the tectonic units of the Korean Peninsula. The average velocities are high and decrease in the following order: YM, OFB, and GB (Jung et al., 2007; Jung et al., 2011; Kim et al., 2011). Although the correlation between velocities and tectonic units was assessed in previous studies, there has been almost no detailed study of the correlation between velocity and geology. The shear-wave velocity increases rapidly down to a few kilometers depth, where the shear-wave velocity is ~3.4 km/s. The depth with a shear-wave velocity of ~3.4 km/s is considered the depth of the top of the basement (Jung et al., 2011). The density and shear modulus play an essential role in examining the shear-

https://doi.org/10.1007/s12303-020-0049-0

wave velocity. The density is dominantly affected by the geologic material and structural conditions (e.g., how much weakening has occurred through fault activity) in the upper few kilometers. The difference in shear-wave velocity in the basement is not caused by differences in the density of geologic materials because the basement consists of geologic materials with similar densities. Therefore, differences in the shear-wave velocity in the basement can be related to the structural conditions and/or shear stress. However, very limited studies have been performed to interpret the reason for differences in shear-wave velocity in the basement.

The shear-wave velocity variations at 1 km depth show a strong correlation with the surface geology in the study area, as mentioned earlier. Low velocities (less than 3.10 km/s) are observed in areas consisting of Cretaceous volcano-sedimentary rocks in the GB and OMB and in Paleozoic metasedimentary rocks in the OMB (Fig. 3a). Velocities greater than 3.14 km/s are clearly associated with the YM, which mainly consists of Precambrian gneisses and Jurassic granites (Figs. 1 and 3a). The shear-wave velocities at depths of 5 and 9 km are higher than 3.4 km/s, and the depths of the Cretaceous volcano-sedimentary unit and Paleozoic metasedimentary unit are shallower than ~3 km (Lee, 1999; Park and Song, 2011). These data indicate that the 5–9 km depth can be regarded as a basement consisting of rather homogeneous density materials. The low velocities in the OMB at this depth generally occur along the faults, suggesting that the low velocities are caused by reductions in the density due to brittle deformation by fault activity. The depth of Cretaceous sedimentary materials in the GB is reported to reach a depth of 8.5 km (Min and Chung, 1985). Therefore, the low velocities observed in the GB can be interpreted to be related to the deep Cretaceous volcano-sedimentary unit. At a depth of 13 km, the shear-wave velocity is almost homogeneous except in the area between the Sunchang and Gwangju faults. The shear-wave velocity at this depth is more homogeneous than that at depths of 5–9 km, indicating that brittle fault movement does not occur at a depth of 13 km. The high shear-wave velocity between the Sunchang and Gwangju faults may be due to relatively high shear stress. These data indicate that the differences in the shear-wave velocities at 1 km depth reflect differences in geology, those at 5–9 km depth reflect areas with and without brittle deformation, and those at 13 km depth reflect differences in shear stress.

In the vertical shear-wave velocity sections (Fig. 4), the 3.5 km/s isovelocity lines show irregular distributions compared to the 3.4 km/s isovelocity lines. In Figure 4b, the 3.5 km/s isovelocity line is deeper in the GB than elsewhere and is irregular with some deeper areas in the OMB, which features many faults. These data suggest that the 3.5 km/s isovelocity line can be deeper in heavily faulted areas and in areas with thick volcano-sedimentary rocks. In Figure 4c, the 3.5 km/s shear-wave velocity line is located at a depth deeper than 7 km in the GM and at a depth deeper than 8–10 km in the eastern OFB, YM, and western GB, where many faults exist. Thus, the areas with velocities less than 3.5 km/s at depths between 5–11 km can be considered to have experienced strong brittle deformation associated with fault activity.

7. CONCLUSIONS

The following conclusions were obtained in this study by comparing earthquakes, faults, geology, and shear-wave velocity tomography in the southwestern Korean Peninsula.

1) Historical earthquakes with magnitudes larger than 5.0 and instrumental earthquakes with magnitudes larger than 3.0 occurred mostly on or near faults.

2) Instrumental earthquakes with focal depths shallower than 12 km generally occurred along faults with NE strikes, while those with focal depths deeper than 12 km generally occurred along faults with NW strikes or showed no relationship with faults. These data suggest that two seismogenic layers exist and have a boundary at ca. 12 km, and a recent earthquake in the Haenam area occurred in the lower seismogenic layer.

3) Differences in the shear-wave velocity at depths shallower than 1 km reflect differences in the rock type in most of the study area.

4) The differences in the shear-wave velocity at depths of 5–9 km reflect the presence or absence of fault zones, in which the density decreases due to the development of cracks induced by faulting, except in the GB, where the depth of sedimentary rocks extends down to 8.5 km.

5) The differences in the shear-wave velocity at a depth of 13 km reflect differences in the shear stress rather than in the rock type or structural conditions.

ACKNOWLEDGMENTS

We would like to thank two anonymous reviewers and editor Kim Kwang-Hee for valuable comments that were helpful in improving our paper.

REFERENCES

Cho, H.M., Baag, C.E., Lee, J.M., Moon, W.I., Jung, H.O., and Kim, K.Y., 2013, P- and S-wave velocity model along crustal scale refraction and wide-angle reflection profile in the southern Korean peninsula. Tectonophysics, 582, 84–100.

Cho, K.H., Takagi, H., and Suzuki, K., 1999, CHIME monazite age of granitic rocks in the Sunchang shear zone, Korea: timing of dextral ductile shear. Geosciences Journal, 3, 1–15.

Choi, H.T. and Kim, T.R., 2018, Necessity of management for minor

earthquake to improve public acceptance of nuclear energy in South Korea. Nuclear Engineering and Technology, 50, 494–503.

Choi, J.H., Kang, T.S., and Baag, C.E., 2009, Three-dimensional surface wave tomography for the upper crust velocity structure of southern Korea using noise correlations. Geosciences Journal, 13, 423–432.

Choi, S.J., Hwang, J.H., Kee, W.S., Kim, Y.B., Choi, B.Y.., Lee, Y.S., Song, K.Y., Kim, Y.H., Kim, H.C., Kim, S.W., Han, J.K., Ryu, C.R., Lee, H.J., Jeon, J.S., Jeon, M.S., Shin, J.S., Sun, C.K., and Kim, G.Y., 2011, Active Fault Map and Seismic Hazard Map. Korea Institute of Geoscience and Mineral Resources, Daejeon, Korea, 688 p.

Chough, S.K., Kwon, S.T., Ree, J.H., and Choi, D.K., 2000, Tectonic and sedimentary evolution of the Korean Peninsula: a review and new view. Earth-Science Reviews, 52, 175–235.

Chung, T.W., Zafar Iqbal, M., Lee, Y.M., Yoshimoto, K., and Jeong, J.N., 2018, Depth-dependent seismicity and crustal heterogeneity in South Korea. Tectonophysics, 749, 12–20.

Herrmann, R.B. and Ammon, C.J., 2002, Computer programs in seismology, Ver. 3.30: Overview, structure. Department of Earth and Atmospheric Sciences, Saint Louis University, Missouri. http://www.eas.slu.edu/People/RBHerrmann/CPS330.html [Accessed on 18 November 2020].

Hong, T.K., Lee, J.H., Park, S.J., and Kim, W.H., 2018, Time-advanced occurrence of moderate-size earthquakes in a stable intraplate region after a megathrust earthquake and their seismic properties. Scientific Reports, 8, 13331.

Houng, S.E. and Hong, T.K., 2013, Probabilistic analysis of the Korean historical earthquake records. Bulletin of the Seismological Society of America, 103, 2782–2796.

Hu, L., Cawood, P.A., Du, Y., Yang, J., and Jiao, L., 2015, Late Paleozoic to Early Mesozoic provenance record of Paleo-Pacific subduction beneath South China. Tectonics, 34, 986–1008.

Jin, K.M., Lee, J.H., Lee, K.S., Kyung, J.B., and Kim, Y.S., 2020, Earthquake damage and related factors associated with the 2016 M_L = 5.8 Gyeongju earthquake, southeast Korea. Geosciences Journal, 24, 141–157.

Jung, H.O., Jang, Y.S., and Jo, B.G., 2011, Upper-crust shear-wave velocity of South Korea constrained by explosion and earthquake data. Bulletin of the Seismological Society of America, 101, 2819–2832.

Jung, H.O., Jang, Y.S., Lee, J.M., Moon, W.I., Baag, C.E., Kim, K.Y., and Jo, B.G., 2007, Shear wave velocity and attenuation structure for the shallow crust of the southern Korean peninsula from short period Rayleigh waves. Tectonophysics, 429, 253–265.

Kang, T.S. and Baag, C.E., 2004, An efficient finite-difference method for simulating 3D seismic response of localized basin structures. Bulletin of the Seismological Society of America, 94, 1690–1705.

Kee, W.S., 2020, An interim result for the Haenam earthquake. Korea Institute of Geoscience and mineral resources, Daejeon, Korea, 8 p.

Kee, W.S., Kim, S.W., Jeong, Y.J., and Kwon, S., 2010, Characteristics of Jurassic continental arc magmatism in South Korea: tectonic implications. The Journal of Geology, 118, 305–323.

Kim, H.W. and Kyung, J.B., 2015, Analysis on the relationship between intencity and magnitude for historical earthquakes in the Korean Peninsula. Journal of Korean Earth Sciences, 36, 643–648.

Kim, K.H., Kang, T.S., Rhie, J., Kim, Y., Park, Y., Kang, S.Y., Han, M., Kim, J., Park, J., Kim, M., Kong, C., Heo, D., Lee, H., Park, E., Park, H., Lee, S.J., Cho, S., Woo, J.U., Lee, S.H., and Kim, J., 2016, The 12 September 2016 Gyeongju earthquakes: 2. Temporary seismic network for monitoring aftershocks. Geosciences Journal, 20, 753–757.

Kim, K.H., Seo, W.S., Han, J.W., Kwon, J., Kang, S.Y., Ree, J.H., Kim, S.S., and Liu, K., 2020, The 2017 M_L 5.4 Pohang earthquake sequence, Korea, recorded by a dense seismic network. Tectonophysics, 774, 228306.

Kim, S.W., Kwon, S., Koh, H.J., Yi, K., Jeong, Y.J., and Santosh, M., 2011, Geotectonic framework of Permo-Triassic magmatism within the Korean Peninsula. Gondwana Research, 20, 865–889.

Kim, S.W., Kwon, S., Park, S.I., Lee, C., Cho, D.L., Lee, H.J., Ko, K., and Kim, S.J., 2016, SHRIMP U-Pb dating and geochemistry of the Cretaceous plutonic rocks in the Korean Peninsula: a new tectonic model of the Cretaceous Korean Peninsula. Lithos, 262, 88–106.

Kim, S.W., Oh, C.W., Choi, S.G., Ryu, I.C., and Itaya, T., 2006, Ridge subduction-related Jurassic plutonism in and around the Okcheon Metamorphic Belt, South Korea, and implications for northeast Asian tectonics. International Geology Review, 47, 248–269.

Kim, S.R., Rhie, J.K., and Kim, G.Y., 2011, Forward waveform modeling procedure for 1-D crustal velocity structure and its application to the southern Korean Peninsula. Geophysical Journal International, 185, 453–468.

Kim, W.H., 1999, P-wave velocity structure of upper crust in the vicinity of the Yangsan Fault region. Geosciences Journal, 3, 17–22.

Lee, B.C., Oh, C.W., Cho, D.L., and Yi, K.W., 2014, Paleoproterozoic magmatic and metamorphic events in the Hongcheon area, southern margin of the Northern Gyeonggi Massif in the Korean Peninsula, and their links to the Paleoproterozoic orogeny in the North China Craton. Precambrian Research, 248, 17–38.

Lee, B.C., Oh, C.W., Cho, D.L., and Yi, K.W., 2019, Paleoproterozoic (2.0–1.97?Ga) subduction-related magmatism on the north–central margin of the Yeongnam Massif, Korean Peninsula, and its tectonic implications for reconstruction of the Columbia supercontinent. Gondwana Research, 72, 34–53.

Lee, B.C., Oh, C.W., Lee, S.H., Seo, J.E., and Yi, K.W., 2020, Ages and tectonic settings of the Neoproterozoic igneous rocks in the Gyeonggi Massif of the southern Korean Peninsula and the correlation with the Neoproterozoic igneous rocks in China. Lithos, 370–371, 105625.

Lee, D.W., 1999, Strike-slip fault tectonics and basin formation during the Cretaceous in the Korean Peninsula. Island Arc, 8, 218–231.

Lee, K.H., 1998, Historical earthquake data of Korea. Journal of the Korean Geophysical Society, 1, 3–22.

Lee, K.H., 2010, Comments on seismicity and crustal structure of the Korean Peninsula. Jigu-Mulli-wa-Mulli-Tamsa, 13, 256–267.

Lee, K.H. and Jin, Y.G., 1991, Segmentation of the Yangsan fault system: geophysical studies on major faults in the Kyeongsang basin. Journal of the Geological Society of Korea, 27, 434–449.

Lee, K.H. and Na, S.H., 1983, A study of microearthquake activity of the Yangsan fault. Journal of the Geological Society of Korea, 19, 127–135.

Lee, K.H. and Yang, W.S., 2006, Historical seismicity of Korea. Bulletin of the Seismological Society of America, 96, 846–855.

Lee, S.G., Masuda, A., Shimizu, H., and Song, Y.S., 2001, Crustal evolution history of Korean Peninsula in East Asia: the significance of

https://doi.org/10.1007/s12303-020-0049-0

Nd, Ce isotopic and REE data from the Korean Precambrian gneisses. Geochemical Journal, 35, 175–187.

Li, S., Suo, Y., Li, X., Zhou, J., Santosh, M., Wang, P., Wang, G., Guo, L., Yu, S., Lan, H., Dai, L., Zhou, Z., Cao, Z., Zhu, J., Liu, B., Jiang, S., Wang, G., and Zhang, G., 2019, Mesozoic tectono-magmatic response in the East Asian ocean-continent connection zone to subduction of the Paleo-Pacific Plate. Earth-Science Reviews, 192, 91–137.

Min, K.D. and Chung, C.D., 1985, Gravity survey on the subsurface structure between Waekwan–Pohang in Kyoungsang Basin. Journal of Korean Institute of Mining Geology, 18, 321–329.

Oh, C.W., 2006, A new concept on tectonic correlation between Korea, China and Japan: histories from the late Proterozoic to Cretaceous. Gondwana Research, 9, 47–62.

Oh, C.W., 2012, The tectonic evolution of South Korea and northeast Asia from Paleoproterozoic to Triassic. Journal of the Petrological Society of Korea, 21, 59–87.

Oh, C.W., Kim, S.W., Ryu, I.C., Okada, T., Hyodo, H., and Itaya, T., 2004, Tectono-metamorphic evolution of the Okcheon Metamorphic Belt, South Korea: tectonic implications in East Asia. Island Arc, 13, 387–402.

Oh, C.W. and Kusky, T., 2007, The Late Permian to Triassic Hongseong-Odesan collision belt in South Korea, and its tectonic correlation with China and Japan. International Geology Review, 49, 636–657.

Oh, C.W., Lee, J.Y., Yengkhom, L., Lee, B.C., and Ryu, H., 2018, Neoproterozoic igneous activity and Permo-Triassic metamorphism in the Gapyeong area within the Gyeonggi Massif, South Korea, and their implication for the tectonics of northeastern Asia. Lithos, 332, 1–19.

Park, J.O. and Song, M.Y., 2011, A study on the gravity anomaly of Okcheon Group based on the gravity measurement around Chung Lake. Journal of the Korean Earth Science Society, 32, 12–20.

Sagong, H., Kwon, S.T., and Ree, J.H., 2005, Mesozoic episodic magmatism in South Korea and its tectonic implication. Tectonics, 24, TC5002.

Ryang, W.H., 2013, Characteristics of strike-slip basin formation and sedimentary fills and the Cretaceous small basins of the Korean Peninsula. Journal of the Geological Society of Korea, 49, 31–45.

Woo, J.U., Rhie, J.K., Kim, S.R., Kang, T.S., Kim, K.H., and Kim, Y.H., 2019, The 2016 Gyeongju earthquake sequence revisited: aftershock interactions within a complex fault system. Geophysical Journal International, 217, 58–74.

Wu, F.-Y., Yang, J.-H., Xu, Y.-G., and Wilde, S., 2019, Destruction of the North China Craton in the Mesozoic. Annual Review of Earth and Planetary Sciences, 12, 173–195.

Yengkhom, K.S., Lee, B.C., Oh, C.W., Yi, K., and Kang, J.H., 2014, Tectonic and deformation history of the Gyeonggi Massif in and around the Hongcheon area, and its implications in the tectonic evolution of the North China Craton. Precambrian Research, 240, 37–59.

Yi, K., Cheong, C.S., Kim, J., Kim, N., Jeong, Y.J., and Cho, M., 2012, Late Paleozoic to Early Mesozoic arc-related magmatism in southeastern Korea: SHRIMP zircon geochronology and geochemistry. Lithos, 153, 129–141.

Zhai, M.G., Zhang, Y.B., Zhang, X.H., Wu, F.Y., Peng, P., Li, Q.L., Hou, Q.L., and Zhao, L., 2016, Renewed profile of the Mesozoic magmatism in Korean Peninsula: regional correlation and broader implication for cratonic destruction in the North China Craton. Science China Earth Sciences, 59, 2355–2388.

Zhou, X.M. and Li, W.X., 2000, Origin of Late Mesozoic igneous rocks in southeastern China: implications for lithosphere subduction and underplating of mafic magmas. Tectonophysics, 326, 269–287.